Mechanical Effect of van der Waals Interactions Observed in Real Time in an Ultracold Rydberg Gas

T. Amthor,[*] M. Reetz-Lamour, S. Westermann, J. Denskat, and M. Weidemüller[†]

Physikalisches Institut, Universität Freiburg, Hermann-Herder-Straße 3, 79104 Freiburg, Germany
(Received 4 July 2006; published 10 January 2007)

We present time-resolved spectroscopic measurements of Rydberg-Rydberg interactions between two Rydberg atoms in an ultracold gas, revealing the pair dynamics induced by long-range van der Waals interactions between the atoms. By detuning the excitation laser, a specific pair distribution is prepared. Penning ionization on a microsecond time scale serves as a probe for the pair dynamics under the influence of the attractive long-range forces. Comparison with a Monte Carlo model not only explains all spectroscopic features but also gives quantitative information about the interaction potentials. The results imply that the interaction-induced ionization rate can be influenced by the excitation laser. Surprisingly, interaction-induced ionization is also observed for Rydberg states with purely repulsive interactions.

Long-range dipolar interactions ubiquitously appear in nature as the cause for binding forces ranging from atomic and molecular gases [1] all the way to large biological systems [2]. Rydberg atoms have attracted much interest in this context, as they represent an ideal system to study quantum dynamics under the influence of dipolar interactions. As a prominent example from cavity quantum electrodynamics, attractive forces between Rydberg atoms and conducting surfaces have been observed as level shifts in atomic beam experiments [3]. Rydberg-atom–Rydberg-atom interactions leading to resonant energy transfer have been studied in thermal beam experiments [4] and later in ultracold Rydberg gases [5,6]. The long-range dipolar interactions can be used to block multiple-Rydberg-atom excitation [7,8] and to create many-particle entangled states, which may be employed for quantum information processing [9,10]. So far, investigations of Rydberg-atom–Rydberg-atom interactions have mainly focused on the electronic degrees of freedom neglecting the center-of-mass motion ("frozen Rydberg gas" [6]). In this Letter, we present real-time measurements of the motion of interacting pairs of Rydberg atoms revealing the character and strength of the long-range interparticle interactions. Our results decisively confirm van der Waals (vdW) interaction to be the primary cause of ionization in an ultracold Rydberg gas.

In most molecular and atomic systems the relevant time-scales of interparticle dynamics are in the sub-ns regime calling for very fast probes. Ultracold atoms bridge to the μs regime as the thermal energy ($T < 1$ mK) is negligible which allows one to study systems with much weaker interactions or large interatomic distances. Because of the negligible kinetic energy, the dynamics of the gas is fully determined by the interatomic interactions. In the case of ground state atoms, time-resolved interactions in a cold sample have been studied using a pump-probe scheme [11] allowing for coherent control of the collision

process [12]. Interaction-induced motion in cold Rydberg gases was recently observed spectroscopically, causing Penning ionization [13] and affecting energy transfer [14]. By combining time-resolved and spectroscopic measurements, we quantitatively examine the vdW interactions between two Rydberg atoms. Our measurements can be directly compared to calculations of induced-dipole inter-action potentials for two Rydberg atoms, which have so far only been performed neglecting spin-orbit coupling [15]. These interaction potentials may even support bound states resulting in the formation of exotic ultralong-range molecules [16].

The idea of the experiment is schematically illustrated in Fig. 1. The vdW interaction between two Rydberg atoms leads to an energy shift of the pair excitation which de-
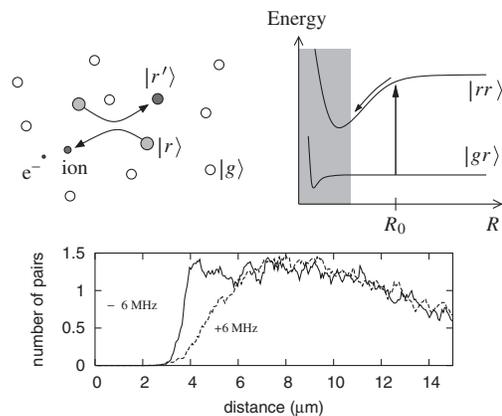
FIG. 1. Excitation and interaction-induced ionization of a pair of atoms on an attractive vdW potential. The atoms are initially excited to state $|r\rangle$ at a distance R_0 by a slightly red-detuned laser. After excitation they are accelerated towards each other and collide, leading to ionization of one of the atoms. The region where this Penning ionization can occur is indicated in gray. The calculated number of pairs excited at specific distances is shown in the lower graph for different detunings.

pends on the pair distance. A red-detuned laser will therefore preferentially excite atoms on an attractive potential in a certain range of distances around an already excited atom. In this way one can use the laser detuning to create a sample with a specific distribution of pair distances. Two examples for $+6$ MHz (blue) and -6 MHz (red) detuning as derived from our model are also plotted in Fig. 1. Once a pair of Rydberg atoms is excited on an attractive potential, the atoms will be accelerated towards each other and collide after a certain time depending on their initial distance R_0. These collisions can lead to Penning ionization. By measuring the number of ions produced after a variable time Δt one can follow the dynamics of the system in real time. The ionization is thus used as a monitor signal for pair dynamics giving quantitative information about the interaction strength.

In our setup we trap ^{87}Rb atoms at temperatures below 100 μK and a peak density on the order of 10^{10} cm^{-3} in a magneto-optical trap (MOT). The atoms are then excited to Rydberg states using a two-photon excitation scheme. The two atomic transitions $5S_{1/2} \rightarrow 5P_{3/2}$ and $5P_{3/2} \rightarrow n\ell$ are realized with two cw laser systems at 780 and 480 nm, respectively. The frequency of the 480-nm excitation laser is actively stabilized using an ultrastable reference cavity. The 480-nm laser is focused to a waist of ~ 37 μm at the center of the MOT with a power of 10 mW. Two metal grids are used to apply electric fields for stray field compensation and for field ionization of the Rydberg states. Ions are detected on a microchannel plate detector. Ref. [17] describes the setup in more detail.

The experimental cycle, repeated every 70 ms, is as follows: The excitation laser is switched on for 100 ns at a given detuning. This time has been chosen sufficiently short so that the movement of the atoms is negligible and no ionization takes place during the excitation. The gas can then evolve freely for a variable time Δt. After that, an electric field ramp is applied to field ionize the Rydberg atoms and accelerate the ions towards the detector. Ions produced by collisions will be drawn to the detector at the very beginning of the ramp (i.e., at low accelerating fields), while Rydberg states ionize at a finite electric field, generating a delayed detector signal. Using two boxcar integrators, the two signals are recorded simultaneously.

Figure 2 shows the Rydberg atom and ion signals at the $60D_{5/2}$ resonance as a function of the excitation laser frequency. The frequency axis is centered at the atomic resonance. In Fig. 2(a) the Rydberg signal measured directly after excitation is displayed. We estimate that the peak signal corresponds to approximately 1000 excited atoms, a few percent of the total number of atoms in the excitation volume. The width of the excitation line is given by a Voigt profile consisting of the Lorentzian width of the intermediate 5P level (6 MHz FWHM), and a Gaussian including the two laser linewidths (2–5 MHz FWHM), the finite excitation time (resulting in a 4.2 MHz FWHM of the Fourier transform), and a ~ 2 MHz broadening due to
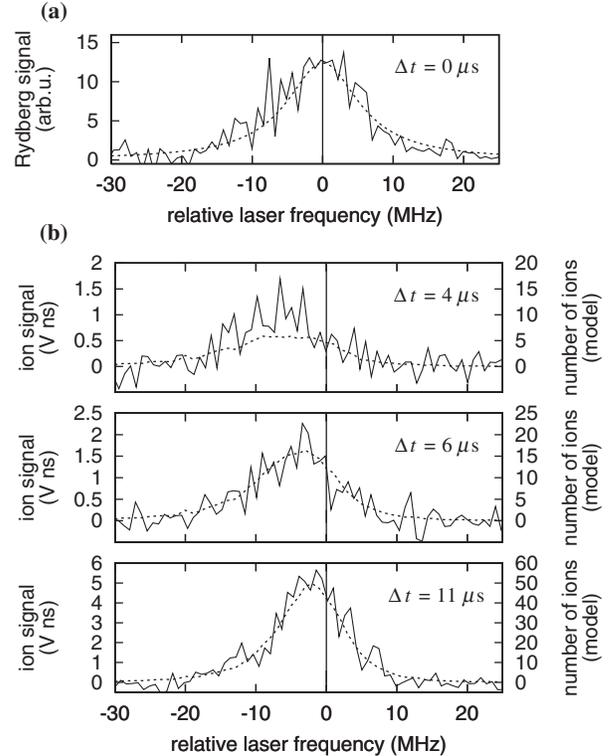
FIG. 2. (a) $60D_{5/2}$ Rydberg excitation line (solid), with fitted Lorentzian (dotted), (b) development of the ion signal for different interaction times (solid) compared to Monte Carlo simulation (dotted). No ions were detected directly after excitation ($\Delta t = 0$). The laser frequency is given relative to the atomic resonance.

residual electric fields. The line shape is still described reasonably well by a Lorentz fit (also shown in the graph) yielding a FWHM of 12.5 MHz as expected from the above numbers. In the graphs in Fig. 2(b) the development of the ion signal after different interaction times Δt is shown. All data are compared to the results of the simulation (dotted lines) described below. Within several μs the number of ions increases steadily. The ion signal peaks at the red-detuned side of the atomic resonance and exhibits a pronounced red wing. As the interaction time increases, most ions appear nearer to the atomic resonance, which can be observed as a shift of the ionization line towards zero detuning. These spectral features can easily be understood in the picture of colliding pairs: After a short interaction time only very close pairs will have had the time to collide, and these pairs are preferentially excited at large detuning. For very long times, the line shape resembles the initial Rydberg excitation line, as almost all atoms are ionized. From these results it is obvious that by slight detuning of the excitation laser the initial ionization rate can be controlled. This can be of importance for applications like quantum computation with Rydberg atoms, where the presence of ions acts as a decoherence process, and for the investigation of ultracold plasma formation.

While a simple analytical description of pair excitations as in Ref. [18] can qualitatively explain the behavior, it

turns out to be insufficient to describe the complex excitation process and thus does not provide quantitative information about the interaction potentials. Instead of considering only the excitation of individual pairs far away from each other our model accounts for the interaction with already excited atoms in the cloud and allows for clustering of Rydberg excitation in order to describe the system more realistically and to reproduce the measured line shapes. We have therefore performed a Monte Carlo simulation. 100 000 atoms are randomly placed in a box with a Gaussian distribution along the excitation laser axis to represent the MOT with a peak density of 1×10^{10} cm^{-3}. Excitation of the gas is described by an iterative procedure: In each iteration step, each of the atoms can be excited with a certain probability. For atom i it is given by $P_i \propto \mathcal{L}[\delta - V(R_i)] \exp[-2(x_i^2 + y_i^2)/w^2]$. $\mathcal{L}$ is the line profile representing the 12.5 MHz linewidth of the Rydberg excitation as described above. $\mathcal{L}$ is evaluated at a detuning consisting of the laser detuning δ and the interaction energy $V(R_i)$ with the nearest Rydberg neighbor to atom i. The Gaussian intensity distribution of the excitation laser with waist $w = 37$ μm is accounted for by the last factor. After each Rydberg excitation, the table of nearest Rydberg neighbors is recalculated for all atoms. This excitation process is iterated to yield the actual excitation fraction of a few percent at the center of the MOT (at zero detuning), and the number of iterations is the same for all detunings.

The excited atoms are then combined to disjoint pairs by successively choosing the two atoms closest to each other. From the resulting list of distances, shown as a histogram in the lower graph in Fig. 1, the number of pairs colliding until a certain time Δt can be determined. We assume an attractive potential of the form $V(R) = -C_6/R^6$. The time it takes a pair of atoms with initial distance R_0 and an initial velocity of zero to collide can then be approximated by the time to reach a distance of zero, $\tau_{\text{coll}} \approx 0.2156 R_0^4 (C_6/m_{\text{Rb}})^{-1/2}$ [18]. To determine the number of ions produced until a time Δt, we count the pairs that collide within this time. The whole simulation is performed for different laser detunings to obtain the line shape of the ion signal. τ_{coll} depends mainly on the long-range part of the potential. It is not significantly affected by variations of the potential at very short distances, e.g., caused by nearby dipole-coupled pair states, which we have checked by calculations. All atoms will eventually ionize, independent of the specific path through short-range potentials, due to the large cross section for this process [19].

The resulting traces shown in Fig. 2 are averaged over 50 random realizations as described above. The best agreement of the Monte Carlo simulation with the experimental results is found for $C_6 = 2 \times 10^{20}$ a.u., while values below 10^{20} and above 10^{21} are not compatible with the measured spectra. This is in agreement with calculations following Ref. [15], yielding exclusively attractive potentials in this range. Note that in the actual experiment an effective potential is observed, which averages over all possible

molecular symmetries. The measured ionization signals [Fig. 2(b)] are well reproduced by the simulation.

While this spectroscopic view shows how the line shape is reproduced by the simulation, one can gain some more insight in the system by comparing the time development of the measured signal and the model at specific detunings, as displayed in Fig. 3. The model predicts a threshold for the ion production at around 3–4 μs, which is also observed in the experiment. Furthermore, when comparing the ionization rates at different detunings relative to each other, we find very similar behavior of model and experiment: At -6 MHz the rate is comparable to the one at zero detuning, while at $+6$ MHz the rate is significantly lower. The error bars at the measured data points display the standard deviation of fluctuations in the signal, while the scale is subject to a systematic error of a factor of 2.

This description will only be applicable as long as collisions between two cold Rydberg atoms are the main cause of ionization. As soon as the ion density becomes sufficiently large to trap electrons, electron–Rydberg-atom collisions will determine the dynamics of the system, causing ionization as well as ℓ and n mixing [20]. We can rule out avalanche ionization during the first few microseconds as the number of ions is not yet sufficient to trap electrons. Redistribution of atoms to other Rydberg states by Penning ionization or by blackbody radiation (estimated rates below 5600 s^{-1} [21]) as well as direct blackbody ionization will also affect the dynamics of the system, but should not have significant influence during the first few μs. For long interaction times, however, we expect our model to become increasingly inaccurate and the measured signal to exceed the simulated one. This is indeed what we observe for $\Delta t > 11$ μs (see Fig. 3).

According to the above analysis one would not expect to see ionization due to inelastic processes when the interaction is repulsive. We have also performed similar measurements for the 60S state, which exhibits only repulsive vdW
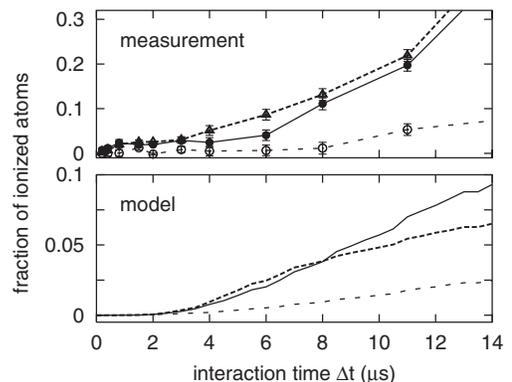
FIG. 3. Signal growth at different detunings: 0 MHz (solid), -6 MHz (triangles, dotted), $+6$ MHz (open circles, dashed). Upper graph: measured data (data points represent bins over 3 MHz), lower graph: model. The scale of the measured data contains a systematic error of a factor of 2 due to different MCP efficiencies for the ion and Rydberg signals.
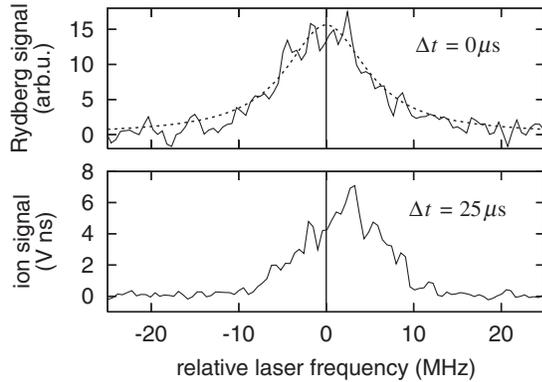
FIG. 4. $60S$ Rydberg excitation spectrum (upper graph) and preionized atoms after 25 μs interaction time (lower graph). The ions are produced on the blue-detuned side of the resonance. Excitation time is 300 ns, and excitation laser power 22 mW. The graphs have different signal height scales. The fit in the upper graph (dotted) yields a line width of 11.3 MHz, similar to the $60D_{5/2}$ line.

interaction [15]. Surprisingly, we still observe ionization, yet only on much longer time scales, as shown in Fig. 4. Most ions are produced on the blue-detuned side of the resonance, which implies that the ionization rate is in conjunction with the repulsive potential. A possible explanation is the redistribution of states due to blackbody radiation leading to attractive dipole-dipole potentials. Atoms initially excited at small distance (i.e., at blue detuning) could then be the first to collide [22]. This process is more difficult to model for a cloud of atoms and a simple approach of including blackbody redistribution and subsequent $1/R^3$ attraction in our Monte Carlo model could not explain the observed line shapes. There may also exist attractive pair potentials of other states crossing the repulsive vdW potentials. Atoms initially repelled from each other may reach a crossing and return on the attractive path. We will further investigate this process in future experiments.

In conclusion, the time-resolved spectroscopic measurements reveal the motion of Rydberg atoms under the influence of van der Waals interactions as the cause of Penning ionization. The temporal evolution of the ionization signal allows one to distinguish van der Waals from resonant dipole interactions. The measured strength of the interaction is in good quantitative agreement with theoretical predictions. The accuracy of determining the interaction strength could be increased by using two excitation laser pulses at different frequencies: The first one to excite a dilute Rydberg gas on the atomic resonance, the second one detuned from resonance to create well-defined pair distributions over a larger range of accessible detunings. Förster resonances may be used to switch the character of the interaction from van der Waals to resonant dipole interaction. In this way our experimental method will allow for a more precise determination of long-range potentials

and challenge refined models of many-body dynamics under the influence of dipolar forces.

*Email address: thomas.amthor@physik.uni-freiburg.de
†Email address: m.weidemueller@physik.uni-freiburg.de

[1] L. Santos, G. V. Shlyapnikov, P. Zoller, and M. Lewenstein, Phys. Rev. Lett. **85**, 1791 (2000).
[2] K. Autumn, Y. A. Liang, S. T. Hsieh, W. Zesch, W. P. Chan, T. W. Kenny, R. Fearing, and R. J. Full, Nature (London) **405**, 681 (2000).
[3] C. I. Sukenik, M. G. Boshier, D. Cho, V. Sandoghdar, and E. A. Hinds, Phys. Rev. Lett. **70**, 560 (1993).
[4] K. Safinya, J. Delpech, F. Gounand, W. Sandner, and T. Gallagher, Phys. Rev. Lett. **47**, 405 (1981).
[5] W. R. Anderson, J. R. Veale, and T. F. Gallagher, Phys. Rev. Lett. **80**, 249 (1998).
[6] I. Mourachko, D. Comparat, F. de Tomasi, A. Fioretti, P. Nosbaum, V. Akulin, and P. Pillet, Phys. Rev. Lett. **80**, 253 (1998).
[7] D. Tong, S. Farooqi, J. Stanojevic, S. Krishnan, Y. Zhang, R. Côté, E. Eyler, and P. Gould, Phys. Rev. Lett. **93**, 063001 (2004).
[8] K. Singer, M. Reetz-Lamour, T. Amthor, L. Marcassa, and M. Weidemüller, Phys. Rev. Lett. **93**, 163001 (2004).
[9] D. Jaksch, J. I. Cirac, P. Zoller, S. L. Rolston, R. Côté, and M. Lukin, Phys. Rev. Lett. **85**, 2208 (2000).
[10] M. D. Lukin, M. Fleischhauer, R. Côté, L. M. Duan, D. Jaksch, J. Cirac, and P. Zoller, Phys. Rev. Lett. **87**, 037901 (2001).
[11] S. D. Gensemer and P. L. Gould, Phys. Rev. Lett. **80**, 936 (1998).
[12] M. Wright, S. Gensemer, J. Vala, R. Kosloff, and P. Gould, Phys. Rev. Lett. **95**, 063001 (2005).
[13] W. Li, P. J. Tanner, and T. F. Gallagher, Phys. Rev. Lett. **94**, 173001 (2005).
[14] A. Fioretti, D. Comparat, C. Drag, T. F. Gallagher, and P. Pillet, Phys. Rev. Lett. **82**, 1839 (1999).
[15] K. Singer, J. Stanojevic, M. Weidemüller, and R. Côté, J. Phys. B **38**, S295 (2005).
[16] C. Boisseau, I. Simbotin, and R. Côté, Phys. Rev. Lett. **88**, 133004 (2002).
[17] K. Singer, M. Reetz-Lamour, T. Amthor, S. Fölling, M. Tscherneck, and M. Weidemüller, J. Phys. B **38**, S321 (2005).
[18] A. Gallagher and D. E. Pritchard, Phys. Rev. Lett. **63**, 957 (1989).
[19] R. E. Olson, Phys. Rev. Lett. **43**, 126 (1979).
[20] A. Walz-Flannigan, J. R. Guest, J.-H. Choi, and G. Raithel, Phys. Rev. A **69**, 063405 (2004).
[21] T. F. Gallagher, *Rydberg Atoms* (Cambridge University Press, Cambridge, England, 1994).
[22] T. F. Gallagher (private communication).